Table S1. dUMP binding to wild-type[a] and C146S TSase at 25 °C

	Wild-type[a]	C146S	C146S-WT
$K_{A,1}$ (M^{-1})[b]	6.0 ± 0.10 x 10^4	3.4 ± 0.3 x 10^3	18-fold
K_{A2} (M^{-1})[b]	5.9 ± 0.10 x 10^4	3.2 ± 0.4 x 10^3	18-fold
$\Delta G°_1$ (kcal/mol)	-6.5 ± 0.1	-4.8 ± 0.1	1.7 ± 0.1 (kcal/mol)
$\Delta G°_2$ (kcal/mol)	-6.5 ± 0.1	-4.8 ± 0.1	1.7 ± 0.1 (kcal/mol)
$\Delta H°_1$ (kcal/mol)	-4.5 ± 0.1	-3.5 ± 0.1	1.0 ± 0.1 (kcal/mol)
$\Delta H°_2$ (kcal/mol)	-4.4 ± 0.1	-3.7 ± 0.1	0.7 ± 0.1 (kcal/mol)
$T\Delta S°_1$ (kcal/mol)	2.0 ± 0.1	1.3 ± 0.1	-0.7 ± 0.1 (kcal/mol)
$T\Delta S°_2$ (kcal/mol)	2.1± 0.1	1.1 ± 0.12	-1.0 ± 0.2 (kcal/mol)
ρ[c]	1.0 ± 0.1	0.9 ± 0.1	-0.1 ± 0.1

[a] Wild-type data reported previously[(1)].

[b] Intrinsic binding constants

[c] Cooperativity constant, ρ, defined as $K_{A,2}/K_{A,1}$

Table S2. Wild-type and C146S Ile, Leu, and Val Methyl S^2_{axis} in free and dUMP-bound TSase

Methyl		WT free S^2_{axis}	WT-dUMP S^2_{axis}	C146S free S^2_{axis}	C146S-dUMP S^2_{axis}
LEU	5 δ1	[a]	0.640 (0.007)[b]		0.682 (0.002)
LEU	5 δ2			0.648 (0.003)	0.697 (0.002)
LEU	7 δ1	0.862 (0.007)	0.926 (0.030)	0.859 (0.011)	0.930 (0.008)
LEU	7 δ2	0.767 (0.004)	0.848 (0.019)	0.774 (0.006)	0.841 (0.005)
VAL	11 γ1	0.832 (0.003)	0.884 (0.013)	0.832 (0.005)	0.905 (0.003)
VAL	11 γ2				0.867 (0.006)
LEU	12 δ1	0.506 (0.002)	0.503 (0.006)	0.503 (0.002)	0.505 (0.001)
LEU	12 δ2	0.479 (0.001)	0.484 (0.005)	0.476 (0.002)	0.484 (0.001)
LEU	27 δ1	0.493 (0.001)	0.348 (0.004)	0.513 (0.001)	0.358 (0.001)
LEU	27 δ2	0.382 (0.001)		0.370 (0.001)	0.366 (0.001)
ILE	29 δ1	0.554 (0.002)	0.603 (0.008)	0.551 (0.002)	0.612 (0.002)
LEU	38 δ1	0.759 (0.005)		0.755 (0.006)	
LEU	38 δ2	0.842 (0.006)	0.815 (0.021)	0.813 (0.008)	0.870 (0.006)
LEU	44 δ1	0.815 (0.003)	0.819 (0.013)	0.802 (0.004)	0.837 (0.003)
LEU	44 δ2	0.824 (0.004)	0.815 (0.014)	0.805 (0.006)	0.831 (0.004)
VAL	45 γ1	0.696 (0.003)	0.692 (0.011)	0.683 (0.004)	0.717 (0.002)
VAL	45 γ2	0.790 (0.003)	0.781 (0.014)	0.777 (0.004)	0.830 (0.003)
LEU	52 δ1	0.230 (0.001)	0.225 (0.005)	0.212 (0.002)	0.230 (0.001)
LEU	52 δ2	0.322 (0.001)	0.320 (0.008)	0.292 (0.002)	0.313 (0.001)
ILE	55 δ1	0.283 (0.002)	0.274 (0.007)	0.320 (0.002)	0.357 (0.002)
ILE	56 δ1	0.859 (0.005)	0.860 (0.021)	0.854 (0.006)	0.895 (0.007)
LEU	59 δ1	0.721 (0.003)			
LEU	59 δ2	0.688 (0.003)		0.729 (0.004)	

LEU	60 δ1				
LEU	60 δ2				
LEU	63 δ1	0.806 (0.003)	0.836 (0.013)	0.801 (0.005)	0.829 (0.003)
LEU	63 δ2	0.893 (0.004)	0.923 (0.016)	0.878 (0.005)	0.913 (0.004)
ILE	69 δ1	0.493 (0.001)	0.498 (0.005)	0.490 (0.001)	0.513 (0.001)
LEU	72 δ1	0.915 (0.005)	0.876 (0.016)	0.868 (0.006)	0.936 (0.005)
LEU	72 δ2	0.884 (0.005)	0.869 (0.016)	0.874 (0.007)	0.905 (0.005)
VAL	77 γ1	0.976 (0.006)		0.956 (0.008)	1.007 (0.006)
VAL	77 γ2	0.906 (0.004)	0.910 (0.013)	0.897 (0.005)	0.923 (0.005)
ILE	79 δ1	0.612 (0.002)	0.615 (0.009)	0.594 (0.002)	0.626 (0.002)
LEU	90 δ1	0.683 (0.003)	0.689 (0.014)	0.648 (0.005)	0.683 (0.005)
LEU	90 δ2	0.620 (0.002)	0.633 (0.010)	0.607 (0.003)	0.631 (0.002)
VAL	93 γ1		0.872 (0.013)	0.874 (0.004)	0.905 (0.003)
VAL	93 γ2	1.011 (0.003)	1.025 (0.014)	1.017 (0.005)	
ILE	109 δ1	0.208 (0.001)	0.204 (0.003)	0.209 (0.001)	0.210 (0.001)
ILE	112 δ1	0.781 (0.005)	0.643 (0.017)	0.782 (0.007)	0.820 (0.006)
VAL	115 γ1	0.901 (0.010)	0.925 (0.031)	0.896 (0.013)	0.927 (0.010)
VAL	115 γ2			0.940 (0.015)	0.976 (0.013)
LEU	116 δ1		0.377 (0.003)		0.601 (0.001)
LEU	116 δ2	0.173 (0.001)	0.169 (0.002)	0.165 (0.001)	0.177 (0.001)
LEU	119 δ1		0.964 (0.020)		0.980 (0.007)
LEU	119 δ2	0.758 (0.007)	0.784 (0.023)	0.756 (0.010)	0.770 (0.008)
ILE	128 δ1	0.842 (0.003)	0.879 (0.012)	0.843 (0.005)	0.880 (0.003)
ILE	129 δ1	0.651 (0.006)	0.498 (0.011)	0.487 (0.003)	0.424 (0.002)
VAL	130 γ1	0.947 (0.006)	0.955 (0.027)	0.953 (0.006)	1.003 (0.005)
VAL	130 γ2	0.862 (0.009)	0.872 (0.030)	0.870 (0.010)	0.867 (0.007)
VAL	135 γ1	0.864 (0.003)	0.860 (0.013)	0.835 (0.004)	0.868 (0.003)
VAL	135 γ2	0.884 (0.005)	0.876 (0.025)	0.875 (0.005)	0.911 (0.004)
LEU	138 δ1			0.468 (0.001)	0.633 (0.002)
LEU	138 δ2	0.581 (0.002)	0.522 (0.008)	0.567 (0.003)	0.548 (0.002)
LEU	143 δ1	0.162 (0.001)	0.209 (0.003)	0.136 (0.001)	0.183 (0.001)
LEU	143 δ2	0.189 (0.001)	0.191 (0.004)	0.149 (0.001)	0.185 (0.001)
VAL	154 γ1	0.834 (0.003)	0.880 (0.010)	0.839 (0.004)	0.891 (0.002)
VAL	154 γ2	0.781 (0.005)	0.839 (0.019)	0.796 (0.006)	0.837 (0.006)
LEU	159 δ1				
LEU	159 δ2				
LEU	163 δ1	0.821 (0.016)	0.859 (0.019)	0.835 (0.007)	0.888 (0.004)
LEU	163 δ2	0.984 (0.004)	1.023 (0.016)	1.006 (0.006)	1.063 (0.004)
VAL	170 γ1	0.621 (0.002)	0.810 (0.013)	0.601 (0.004)	0.800 (0.003)
VAL	170 γ2	0.687 (0.004)	0.937 (0.021)	0.672 (0.005)	0.887 (0.006)
LEU	172 δ1	0.289 (0.001)		0.316 (0.001)	0.433 (0.001)
LEU	172 δ2	0.340 (0.001)		0.374 (0.002)	0.494 (0.001)
LEU	174 δ1	0.909 (0.010)	0.938 (0.031)	0.889 (0.008)	0.965 (0.006)

LEU	174 δ2	0.848 (0.006)	0.894 (0.023)	0.843 (0.008)	0.885 (0.007)
ILE	178 δ1	0.709 (0.002)	0.757 (0.008)	0.702 (0.003)	0.778 (0.002)
LEU	183 δ1				0.324 (0.001)
LEU	183 δ2	0.191 (0.001)	0.191 (0.003)	0.189 (0.002)	0.191 (0.001)
LEU	184 δ1	0.730 (0.004)	0.758 (0.014)	0.733 (0.007)	0.776 (0.005)
LEU	184 δ2	0.742 (0.004)	0.777 (0.012)	0.794 (0.005)	0.816 (0.003)
VAL	185 γ1	0.801 (0.002)	0.806 (0.005)	0.813 (0.003)	0.833 (0.002)
VAL	185 γ2	0.883 (0.004)	0.870 (0.009)	0.897 (0.004)	0.932 (0.003)
LEU	194 δ1	0.833 (0.005)	0.862 (0.017)	0.824 (0.007)	0.861 (0.006)
LEU	194 δ2				0.912 (0.003)
VAL	196 γ1	0.881 (0.005)	0.867 (0.013)	0.879 (0.006)	0.901 (0.005)
VAL	196 γ2	0.942 (0.003)	0.895 (0.010)	0.932 (0.004)	
VAL	200 γ1	0.944 (0.003)	0.938 (0.010)	0.945 (0.004)	0.983 (0.003)
VAL	200 γ2	0.919 (0.002)	0.907 (0.011)	0.915 (0.004)	0.951 (0.002)
LEU	208 δ1	0.368 (0.001)	0.723 (0.010)	0.385 (0.003)	0.717 (0.003)
LEU	208 δ2		0.756 (0.015)		0.736 (0.003)
LEU	218 δ1	0.474 (0.001)	0.495 (0.006)	0.475 (0.002)	0.534 (0.001)
LEU	218 δ2	0.535 (0.002)		0.539 (0.002)	
LEU	220 δ1	0.745 (0.002)	0.762 (0.010)	0.740 (0.004)	0.775 (0.003)
LEU	220 δ2	0.760 (0.003)	0.757 (0.013)	0.745 (0.005)	0.723 (0.003)
LEU	227 δ1				
LEU	227 δ2				
LEU	230 δ1	0.643 (0.003)	0.650 (0.011)	0.633 (0.004)	0.671 (0.003)
LEU	230 δ2	0.701 (0.004)	0.718 (0.015)	0.696 (0.006)	0.742 (0.005)
ILE	231 δ1	0.185 (0.001)	0.189 (0.003)	0.180 (0.001)	0.185 (0.001)
ILE	232 δ1	0.895 (0.004)	0.898 (0.013)	0.893 (0.005)	0.940 (0.004)
ILE	239 δ1	0.224 (0.001)	0.233 (0.003)	0.223 (0.001)	0.230 (0.001)
ILE	249 δ1	0.128 (0.001)	0.126 (0.002)	0.127 (0.001)	0.128 (0.001)
ILE	258 δ1	0.972 (0.003)	0.997 (0.016)	0.969 (0.004)	1.017 (0.004)
VAL	262 γ1	0.079 (0.001)	0.088 (0.001)	0.083 (0.001)	0.098 (0.001)
VAL	262 γ2	0.084 (0.001)	0.101 (0.001)	0.088 (0.001)	0.114 (0.001)
ILE	264 δ1	0.083 (0.001)	0.096 (0.002)	0.088 (0.001)	0.098 (0.001)

[a] Empty cells correspond to either unassigned or overlapped resonances.

[b] Errors are in parentheses.

Table S3. Raltitrexed binding to the C146S-dUMP complex by ITC

	$K_{A,1}$ (M^{-1})[a]	$K_{A,2}$ (M^{-1})[a]	$\Delta H°_1$ (kcal/mol)	$\Delta H°_2$ (kcal/mol)	ρ[b]
5 °C	5.1 ± 1.3 x 10^5	6.5 ± 2.2 x 10^5	3.3 ± 0.1	2.9 ± 0.1	1.3 ± 0.3
15 °C	1.3 ± 0.4 x 10^6	9.5 ± 4.3 x 10^5	-1.0 ± 0.1	-1.6 ± 0.1	0.7 ± 0.4
25 °C	1.9 ± 1.0 x 10^6	8.7 ± 6.2 x 10^5	-5.2 ± 0.1	-5.6 ± 0.1	0.5 ± 0.4

[a] Intrinsic binding constants

[b] Cooperativity constant, ρ, defined as $K_{A,2}/K_{A,1}$

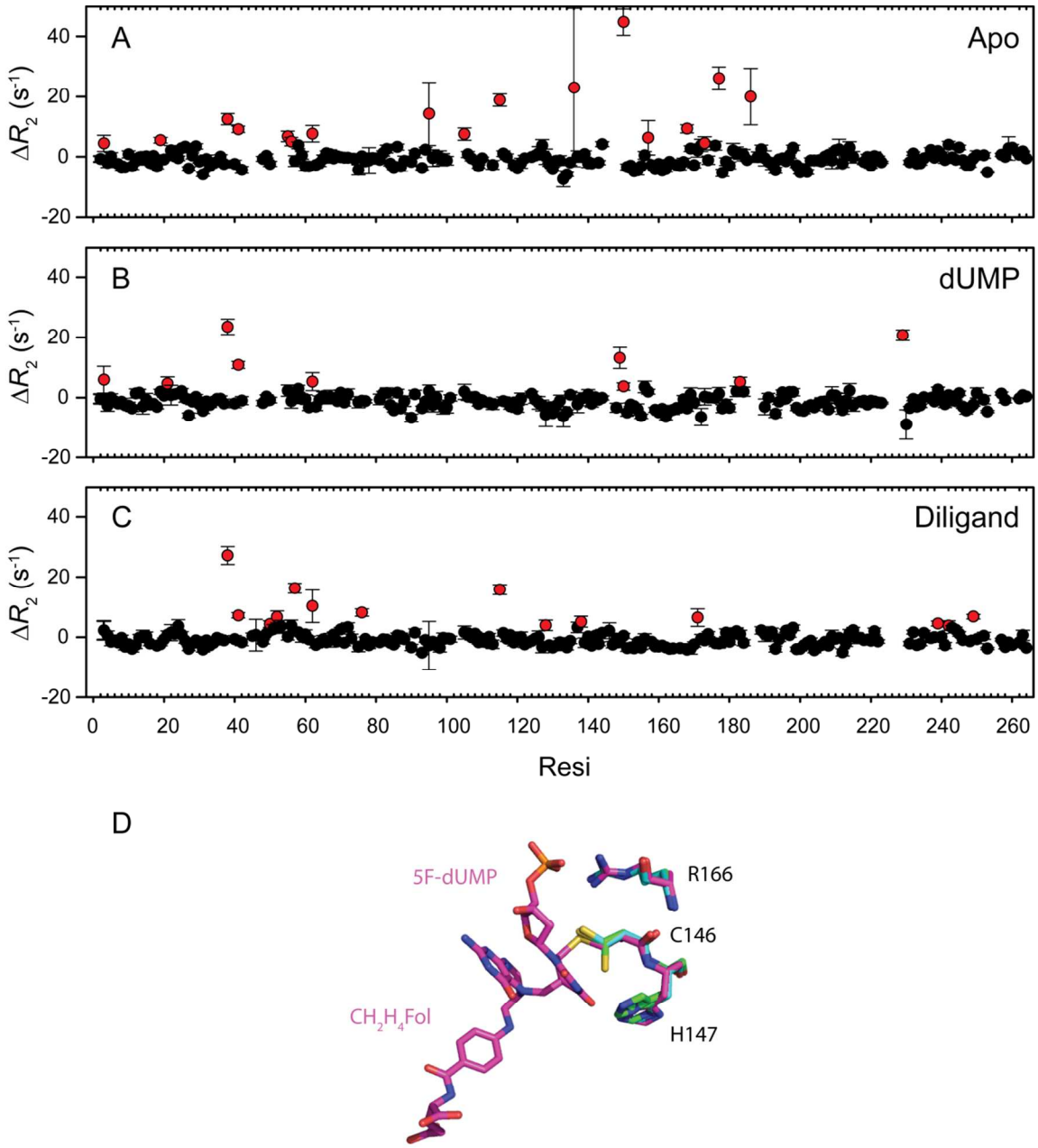

Figure S1. Difference in Hahn-echo ^{15}N transverse relaxation rates (850 MHz – 600 MHz) reporting on µs-ms motions (R_{ex}) for three states along the TSase relaxation coordinate. Data are shown for the free (A), dUMP-bound (B), and 5F-dUMP CH_2H_4-Fol diligand-bound TSase (C). Residues with significant R_{ex} were identified using box-plots (See experimental Procedures). The catalytic C146 and nearby residues are undergoing µs-ms motion in the first two states as evidenced by missing resonances and elevated ΔR_2 values (Panels A&B). This R_{ex} is quenched in the diligand complex (Panel C). Panel D shows three active site residues (C146, H147, and R166) for the Apo (CPK coloring with green carbon), dUMP (CPK coloring with cyan carbon), and diligand (CPK coloring with magenta carbon) states. Note the two conformations of C146 and H147 in the Apo state, which is consistent with our observation that these resonances are broadened away in the free state. However, as we state in the main manuscript, resonances for C146 and H147 are also broadened away in the dUMP state yet the x-ray model shows a single conformation. Thus, there could be other contributors to the R_{ex}.

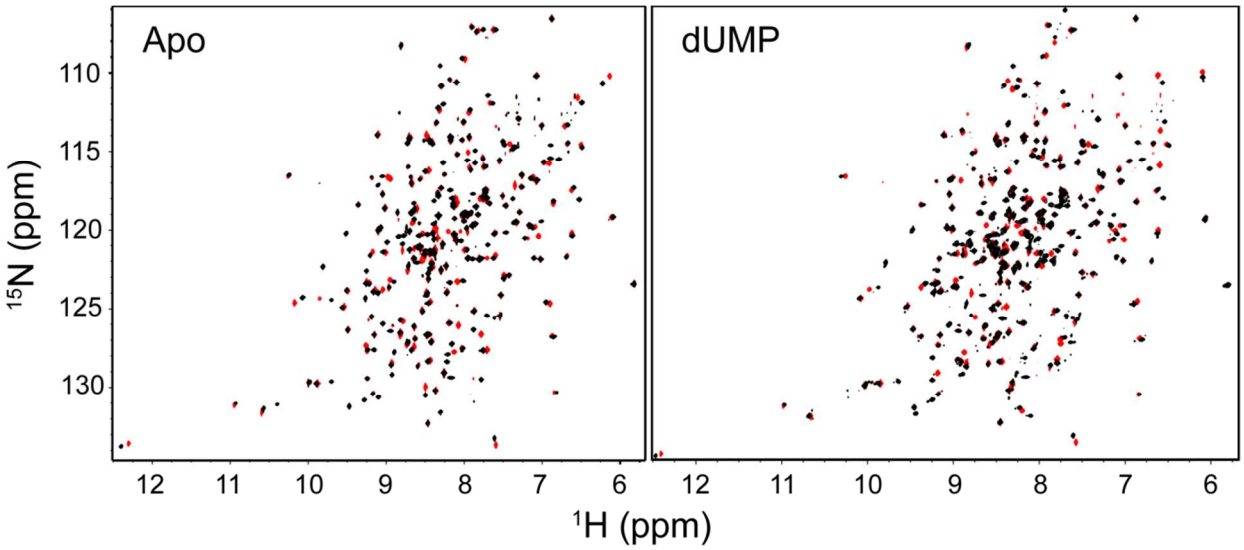

Figure S2. TROSY ^{1}H-^{15}N HSQCs of wild-type (black) and C146S (red) TSase. Spectra of the free enzymes are on the left and spectra of the dUMP complex are on the right. These resonance positions were used to generate Figure 4.

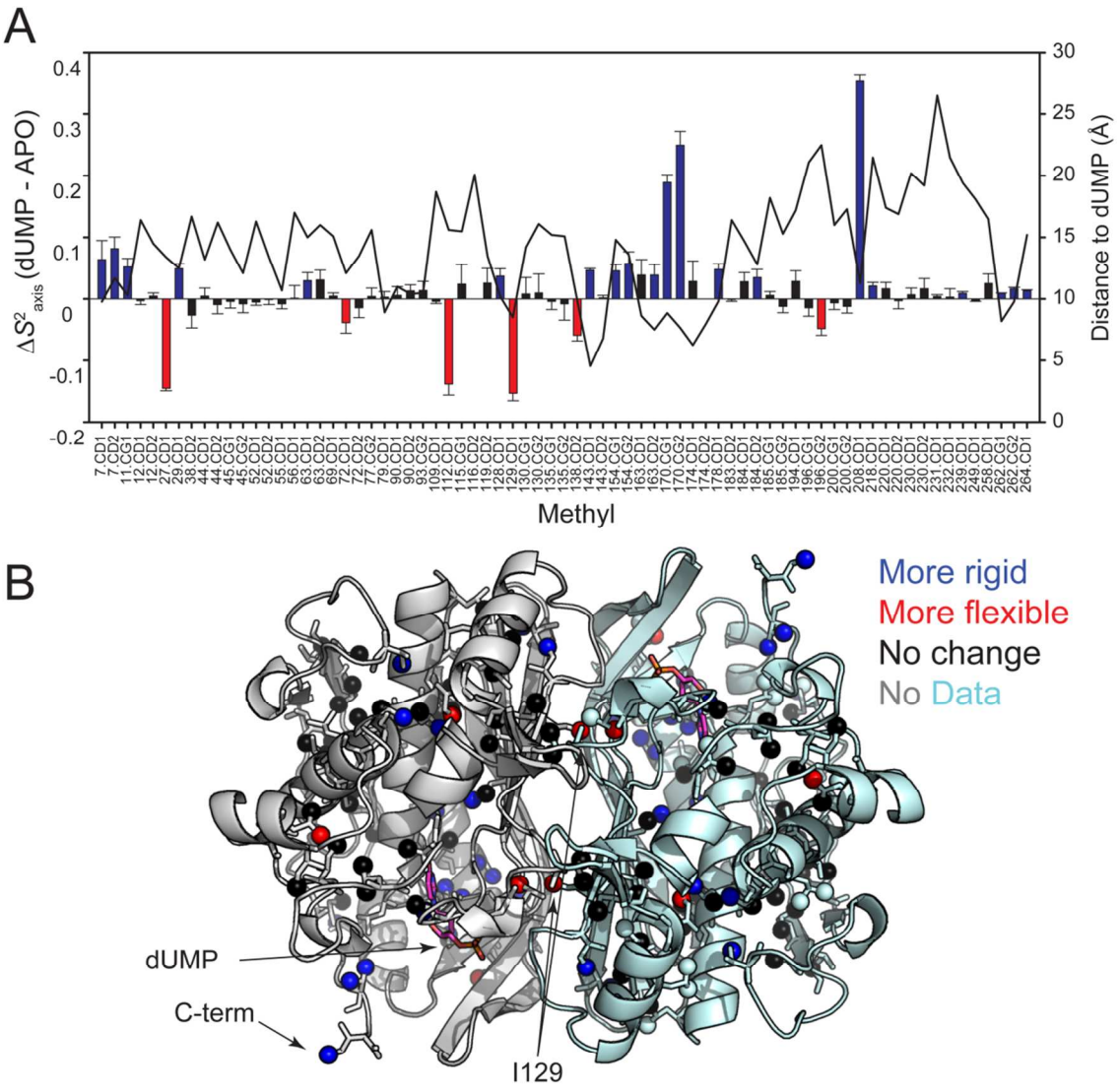

Figure S3. Changes in TSase S^2_{axis} upon dUMP binding. (A) Significant (2σ) changes in ΔS^2_{axis} are colored blue for rigidification and red for increased flexibility. Probes with no significant change are colored black. The line plot associated with the right y-axis refers to the distance between a pseudoatom placed at the average position of the three methyl protons and the nearest dUMP atom in either binding site in the 1BID x-ray model. (B) ILV methyl probes are colored according to the scheme described from panel A. The probes lacking data due to resonance overlap are colored grey and cyan for the first and second subunit, respectively.

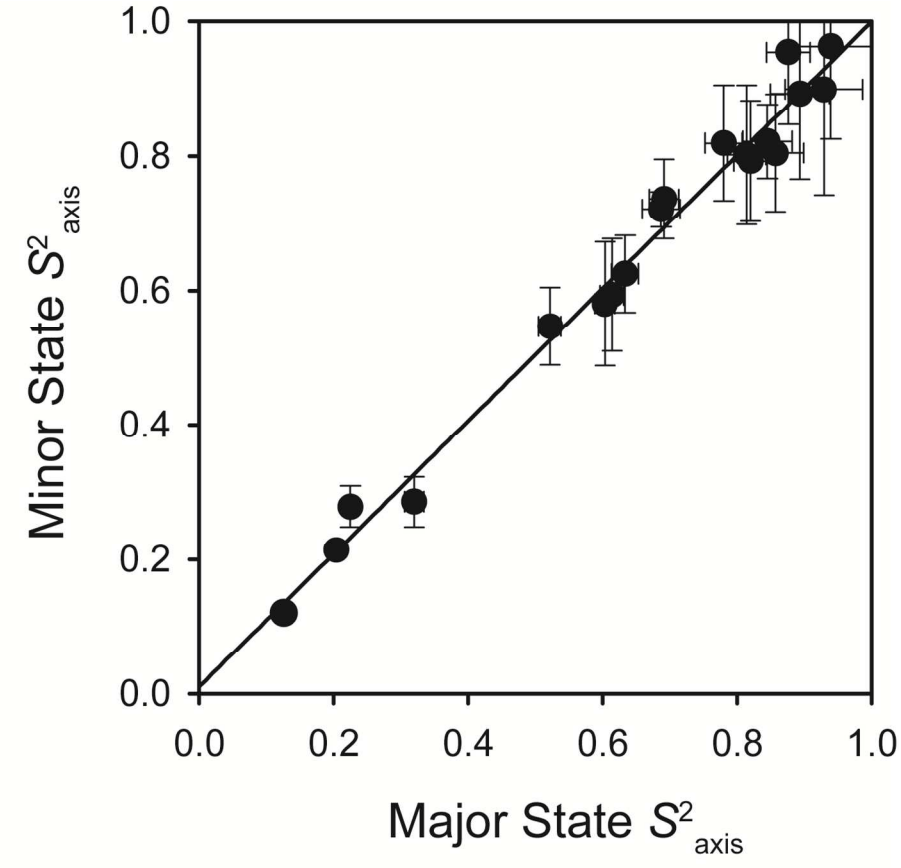

Figure S4. Covalent bond between C146 and dUMP does not affect methyl dynamics. Methyl order parameters, S^2_{axis}, for the 19 probes that have resonances for the major state (non-covalent dUMP complex) and minor state (covalent bond between C146 and C6 of dUMP). The line is best fit to the data with slope of 0.99 and intercept of 0.01.

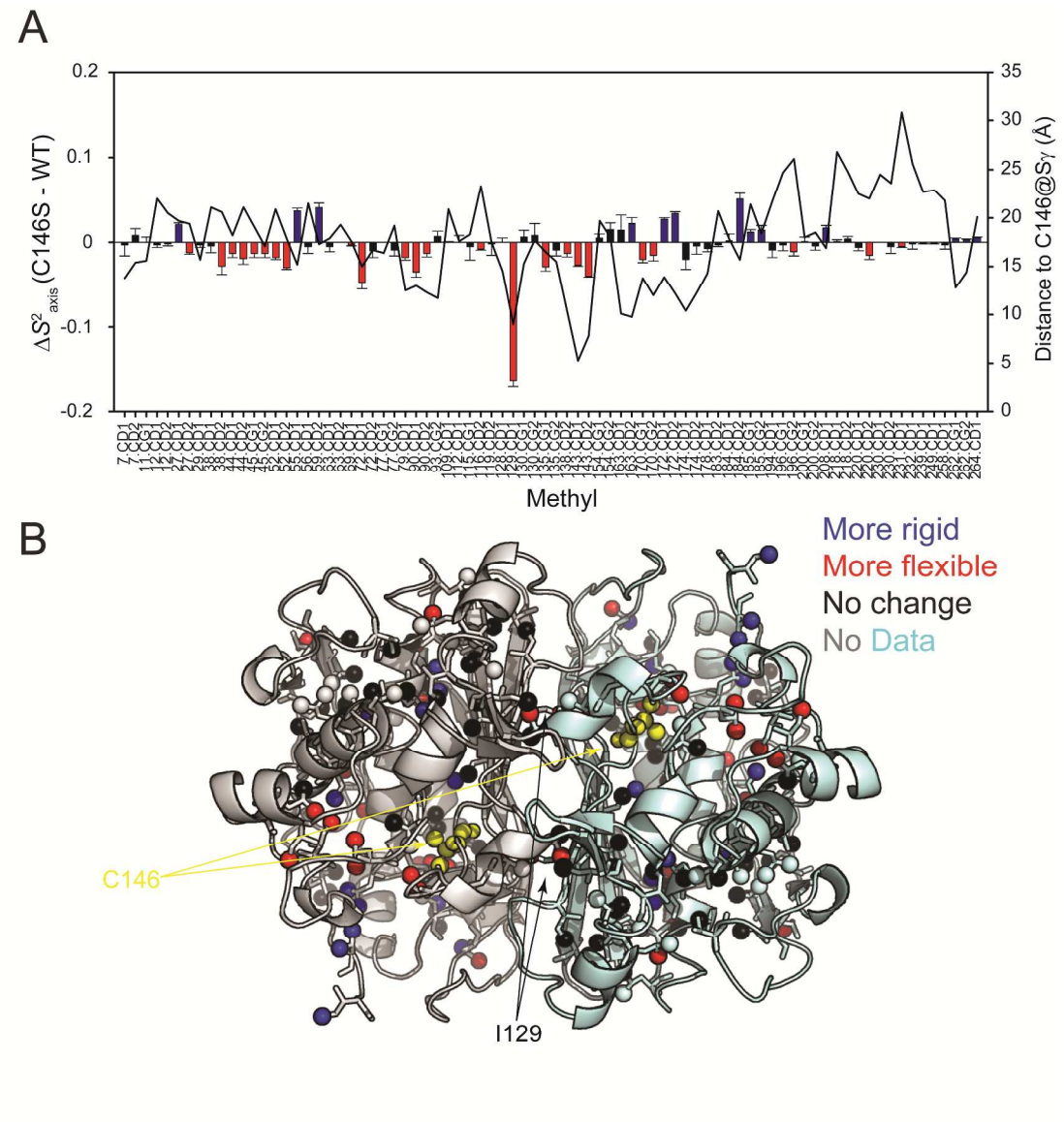

Figure S5. Effect of C146S mutation on Apo TSase S^2_{axis}. Changes in free TSase S^2_{axis} due to the C146S mutation. (A) Significant (2σ) changes in ΔS^2_{axis} are colored blue for rigidification and red for increased flexibility. Probes with no significant change are colored black. The line plot associated with the right y-axis refers to the distance between a pseudoatom placed at the average position of the three methyl protons and C146@Sγ in the 2FTQ x-ray model. (B) ILV methyl probes are colored according to the scheme described from panel A. The probes lacking data due to resonance overlap are colored grey and cyan for the first and second subunit, respectively.

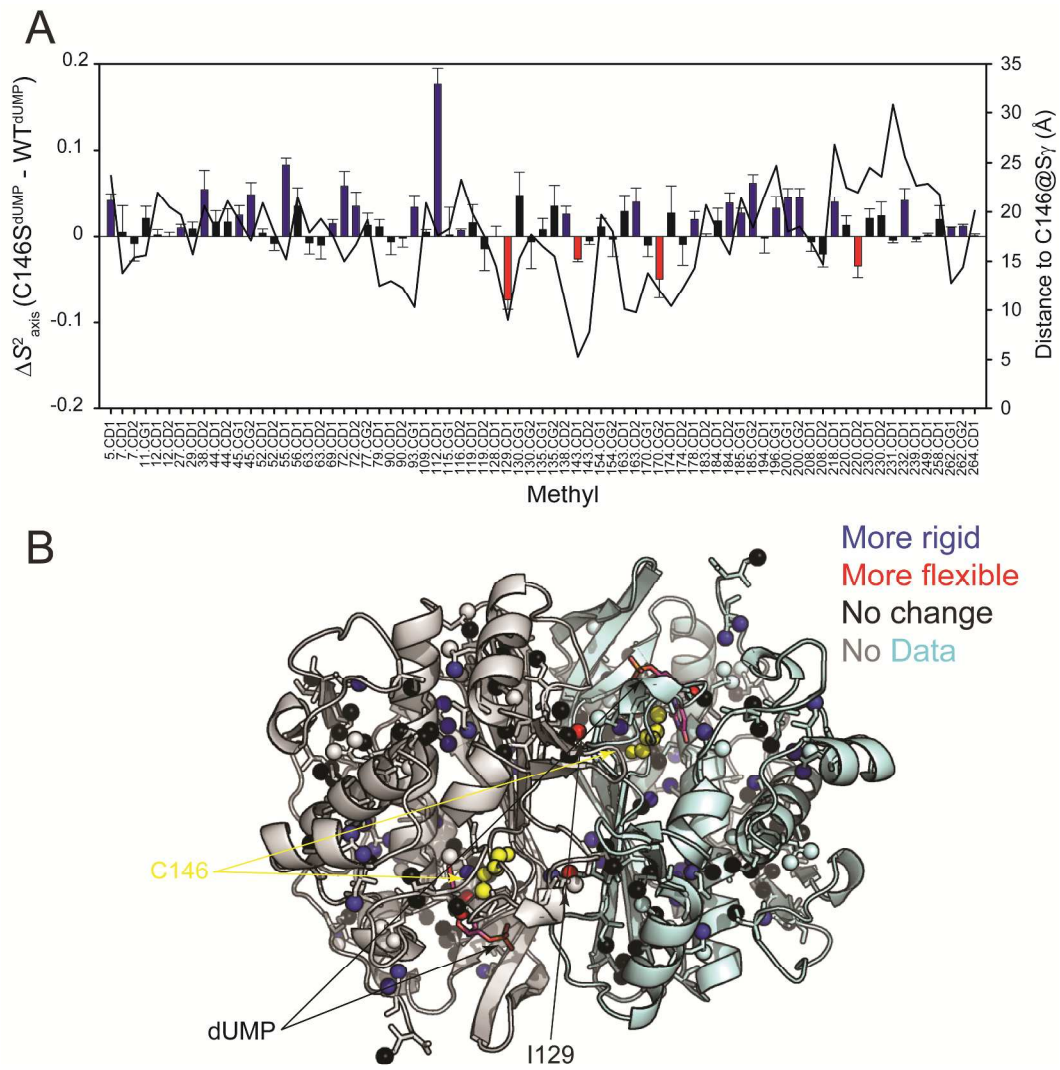

Figure S6. Effect of C146S mutation on TSase-dUMP S^2_{axis}. Changes in TSase-dUMP S^2_{axis} due to the C146S mutation. (A) Significant (2σ) changes in ΔS^2_{axis} are colored blue for rigidification and red for increased flexibility. Probes with no significant change are colored black. The line plot associated with the right y-axis refers to the distance between a pseudoatom placed at the average position of the three methyl protons and C146@Sγ in the 2FTQ x-ray model. (B) ILV methyl probes are colored according to the scheme described from panel A. The probes lacking data due to resonance overlap are colored grey and cyan for the first and second subunit, respectively.

1. Sapienza, P. J., Falk, B. T., and Lee, A. L. (2015) Bacterial Thymidylate Synthase Binds Two Molecules of Substrate and Cofactor without Cooperativity, *J Am Chem Soc 137*, 14260-14263.